

Lateral Control of a Convoy of Autonomous and Connected Vehicles with Limited Preview Information

Mengke Liu, *Member, IEEE*, Sivakumar Rathinam, *Senior Member, IEEE*, and Swaroop Darbha, *Fellow, IEEE*

Abstract— This paper deals with the lateral control of a convoy of autonomous and connected following vehicles (ACVs) for executing an Emergency Lane Change (ELC) maneuver. Typically, an ELC maneuver is triggered by emergency cues from the front or the end of convoy as a response to either avoiding an obstacle or making way for other vehicles to pass. From a safety viewpoint, connectivity of ACVs is essential as it entails obtaining or exchanging information about other ACVs in the convoy. This paper assumes that ACVs have reliable connectivity and that every following ACV has the information about GPS position traces of the lead and immediately preceding vehicles in the convoy. This information provides a “discretized” preview of the trajectory to be tracked. Based on the available information, this article focuses on two schemes for synthesizing lateral control of ACVs based on (a) a single composite ELC trajectory that fuses lead and preceding vehicle’s GPS traces and (b) separate ELC trajectories based on preview data of preceding and lead vehicles. The former case entails the construction of a single composite ELC trajectory, determine the cross-track error, heading and yaw rate errors with respect to this trajectory and synthesize a lateral control action. The latter case entails the construction of two separate trajectories corresponding to the lead vehicle’s and preceding vehicle’s data separately and the subsequent computation of two sets of associated errors and lateral control actions and combining them to provide a steering command. Numerical and experimental results corroborate the effectiveness of these two schemes.

I. INTRODUCTION

Connectivity is an important attribute of Autonomous and Connected Vehicles (ACVs) and can be exploited to enhance safety and mobility in normal and abnormal driving situations. An Emergency Lane Change (ELC) scenario (shown in Figure 1) can be used to illustrate how connectivity can be exploited to enhance traffic mobility and safety. In this scenario, a convoy of ACVs encounters an obstacle (in the Figure 1, it is located on the left side of the right lane of a 2-lane highway) and execute an ELC maneuver as a collision-avoidance measure. Since the line of sight of the obstacle from the ego vehicle (i_{th} ACV as shown in Figure 1) can be occluded by its predecessors (such as the i_{th} ACV and its predecessors shown by the dotted

rectangles), it is possible that safety can be compromised if ACVs are deprived of connectivity and if they do not maintain a sufficiently large following distance; it is possible that the distance, Δ_{i-1} at which the $(i-1)^{st}$ ACV has the obstacle in its line of sight for the first time can be higher than the corresponding value, Δ_i , for the i_{th} ACV. Connectivity on the other hand will enable not ACVs to not only exchange the information about the location of the obstacles but also their own state information to other ACVs and the infrastructure.

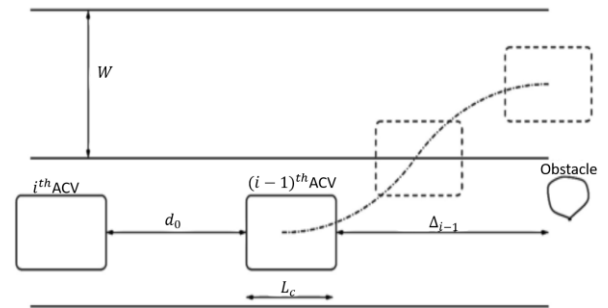


Fig. 1. ELC Scenario

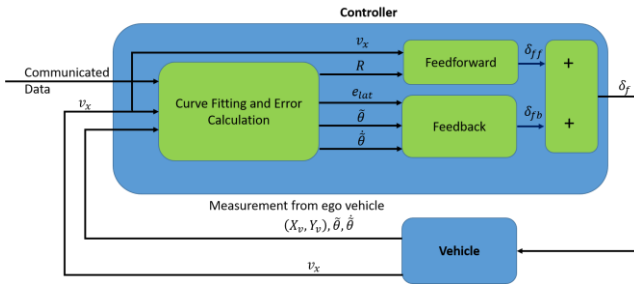
Often, lateral control of ACVs is heavily dependent on the road infrastructure [1] via a reference wire [2] or magnets [3] or signals embedded in the road or by lane markers [4]. This dependence on road infrastructure makes the system expensive and vulnerable to weather conditions, especially in the presence of snow or smog. If driving situations demand close following distances (for example, for eco-driving), it may not be possible to detect lane markings on the road. In defense applications, a ready road infrastructure may not be available for convoying [5]. During an ELC maneuver, the road infrastructure (in terms of lane markings or embedded magnets) may not be as useful as it would be during lane keeping. Hence, there is a need for developing lateral control schemes that do not depend on road infrastructure but can exploit connectivity.

In this paper, we address the problem of lateral control of a convoy of ACVs that exploits connectivity to execute an ELC

Mengke Liu is a doctoral candidate in Mechanical Engineering at Texas A&M University, College Station, TX 77843, USA; e-mail: liu1989@tamu.edu

Siva Rathinam and Swaroop Darbha are faculty members in the Mechanical Engineering at Texas A&M University, College Station, TX 77843-3123, USA; e-mail: srathinam, dswaroop@tamu.edu

maneuver. At any instant of time, each ACV knows its position, heading and heading rate in a ground frame and its longitudinal speed, and can communicate this information to other ACVs in the convoy. By connectivity, we assume that each *following* ACV has the information of the communicated position information of lead ACV and its immediately preceding ACV (see Communicated Data Input in Figure 2). The challenge faced by each following ACV is threefold: (1) it must determine a "target" trajectory to track based on the available sensed/communicated information, (2) it must then determine the feedforward steering command via determining the curvature of the trajectory and (3) compute error signals with respect to the target trajectory and compute a feedback control action that regulates the trajectory of ACV to the target trajectory. Error signals that reflect the performance of the controller include cross track error (distance of the ACV from the closest point on target trajectory), heading error (deviation of the heading of the ACV from the direction of the tangent to the target trajectory at the closest point on the target trajectory) and heading error rate. A schematic of the architecture for the proposed lateral controller addressing the above challenges in this paper is given in the figure 2.



It has been recognized that cross track errors can amplify from one ACV to its following ACV if every ACV relies only on the information from its preceding ACV [5][6][7]; this situation is akin to the longitudinal control case [8]. In order to suppress string instability, a practical solution advocated in [6] is to exploit inter-vehicular communication. In this paper, position, heading and heading rate information of the lead ACV is communicated to every following ACV in the convoy -- this is similar to the California PATH architecture for longitudinal control [8]. Since ACVs need not be identical, communicating vehicle-specific information such as throttle angle, steering angle or brake pedal position information may not be suitable; hence, it is simpler from the implementation viewpoint to focus on communicating information about vehicle kinematics. While the proposed architecture is similar in spirit to the longitudinal vehicle following architecture employed by California PATH [6][7][8][9][10], the details of how the lead vehicle information is used is markedly different as can be seen in the following sections.

A. Relation to Literature & Novelty of the proposed work

A brief review of lane changing maneuvers and associated control schemes can be found in [11][12][13]. The proposed work is solely based on (a) GPS/IMU measurements of ego vehicle's position, heading, heading rate and longitudinal

velocity (see the outputs of vehicle block in Figure 2) and (b) on communicated position information from lead and preceding vehicles. This is in sharp contrast to the use of vision [4] or magnetometers [6][14] or a guided wire [2]. The idea of using history (or trace) information of the position of preceding vehicles was considered in [9]; the authors only consider a two vehicle platoon with Ackerman steering input only; they do indicate the need for refining the dynamic model. The proposed work contrasts with this work in the use of a dynamic model that accounts for lateral acceleration at high speeds and considers multiple vehicle convoys. Lu and Tomizuka [6] advocate the issue of inter-vehicular communication to suppress string instability; the control structure in [6] is different owing to sensing. Specifically, Lu and Tomizuka [6] try to match the position of a rigid extension of its front bumper in the longitudinal direction to the position of the back bumper in the longitudinal direction of the immediately preceding vehicle; additionally, their controller uses magnetometer for sensing the lateral deviation. Recently, Ploeg and his collaborators [1][7] considered the lateral control of a convoy. Alleleijn et al [1] recommend communicating lateral acceleration for alleviating string instability concerns by enforcing a condition on the propagation transfer function of the rate of change of heading angle of the preceding vehicle. In [10], a \mathcal{H}_∞ controller is employed as against a static output feedback controller proposed here.

Literature on lateral control of vehicles [6], [7], [14][15][16][17] has considered the closed loop system to be a linear time-invariant system. In some of the references, authors have included time varying nature of longitudinal speed as an uncertainty and have designed loop-shaping or \mathcal{H}_∞ controllers for robustifying their control design. In this paper, we use a frozen parameter approach - i. e., find the stabilizing set of controllers for a constant longitudinal speed; find controller that lies in the intersection of the stabilizing set of controllers for a range of operational longitudinal speeds. Since longitudinal speed of an ACV can change (however slowly it may be) with time, there is a question of the stability of closed loop system with time varying longitudinal speed which we address in this paper.

The *novel* contributions of this paper are (a) to provide a direct method to fuse the information of the lead and preceding vehicles to synthesize target trajectories that aid lateral string stability by suppressing the amplification of cross track errors, and (b) to corroborate numerically and experimentally the performance of the lateral controller using the feedback controller synthesized in the earlier work of the authors [5], [17]. An additional novel contribution of this paper is to demonstrate that the frozen parameter controller design approach guarantees closed loop stability if (a) the longitudinal speed of ACV exceeds a certain non-zero threshold and is upper bounded, (b) its longitudinal acceleration is square integrable. This is reasonable given the finite duration of ELC maneuvers.

B. Organization

The paper is organized as follows: In section II, we briefly discuss the vehicle model. In section III, we present the lateral control schemes; in section IV, we will present experimental and simulation results and provide summary and concluding remarks in section V.

II. MATHEMATICAL MODEL FOR LATERAL DYNAMICS OF AN ACV

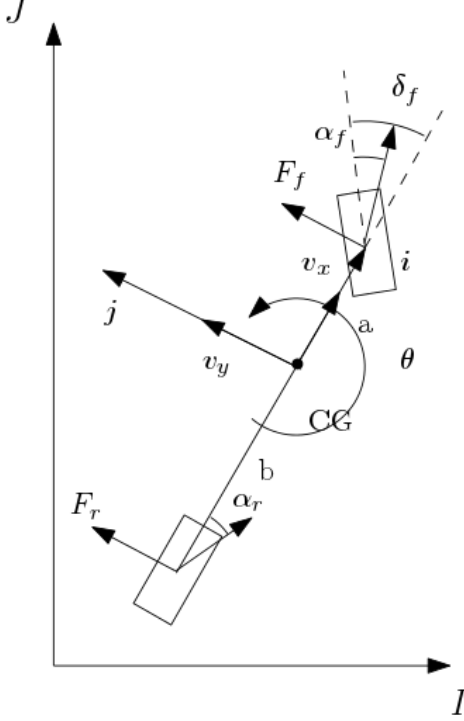


Fig. 3: Illustration of bicycle model

The standard "bicycle" model has been the primary basis for lateral vehicle control [7], [14], [17]-[23]. Let m, I_z be the vehicle mass and moment of inertia about its center of mass, C_f, C_r be the cornering stiffness of the front and rear tires respectively, a, b be the distance of the center of mass to the front and rear axles respectively. For a front-steered vehicle with steering input, δ_f , application of Newton-Euler's equations, along with linear constitutive equations for cornering forces from the tires, yields the following equations of motion:

The last two equations can be simplified as:

$$m \left(\frac{dv_y}{dt} + v_x \dot{\theta} \right) = C_f \delta_f - \frac{C_f + C_r}{v_x} v_y - \frac{aC_f - bC_r}{v_x} \dot{\theta} \quad (1)$$

$$I \dot{\theta} = aC_f \delta - \frac{aC_f - bC_r}{v_x} v_y - \frac{a^2 C_f + b^2 C_r}{v_x} \dot{\theta} \quad (2)$$

For feedback controller design, it is desired to cast the equations of motion using errors in position and heading with respect to the desired trajectory. Based on the previous work [17][24].

We can express vehicle dynamic equations (1) and (2) in terms of the states, $e_{lat}, \dot{e}_{lat}, \tilde{\theta}, \frac{d\tilde{\theta}}{dt}$ using the following matrices:

$$\mathbf{M} := \begin{bmatrix} m & 0 \\ 0 & I_z \end{bmatrix}, \mathbf{C} := \begin{bmatrix} \frac{C_f + C_r}{V_0} & \frac{aC_f - bC_r}{V_0} \\ \frac{aC_f - bC_r}{V_0} & \frac{a^2 C_f + b^2 C_r}{V_0} \end{bmatrix} \quad (3)$$

$$\mathbf{B} := \begin{bmatrix} 1 \\ a \end{bmatrix}, \quad \mathbf{F} := mV_0^2(aC_f - bC_r) \quad (4)$$

$$\mathbf{L} := \begin{bmatrix} 0 & -(C_f + C_r) \\ 0 & -(aC_f - bC_r) \end{bmatrix}, \mathbf{x} := \begin{bmatrix} e_{lat} \\ \tilde{\theta} \end{bmatrix} \quad (5)$$

Governing equations thus can be written as:

$$\mathbf{M}\ddot{\mathbf{x}} + \mathbf{C}\dot{\mathbf{x}} + \mathbf{L}\mathbf{x} = \mathbf{B}C_f\delta_f - \mathbf{F}\left(\frac{1}{R}\right). \quad (6)$$

Based on our previous work [24], we use an experimentally corroborated second order model for steering actuation dynamics; a similar model was used in [7]. The actuation transfer function is given by:

$$H_a(s) = \frac{w_n^2}{s^2 + 2\zeta w_n s + w_n^2}$$

where J_w is the steering wheel inertia, b_w is the torsional viscous damping coefficient and K_r is the torsional stiffness of the steering column; the input to the transfer function is the steering angle command to MKZ vehicle. We found that $\zeta = 0.4056$, from the data; these values compare with similar values of $\zeta = 0.7$ and $\omega_n \approx 19$ rad/sec used in [7]. We use the $\omega_n = 21.4813$ rad/s values for design and implementation of lateral controller.

Below is the table of parameters we have determined experimentally [17], [24]. In this table, $m = \frac{W}{g}$.

TABLE I
PARAMETERS OF VEHICLE

Parameter	Description	Value	Unit
m	Vehicle total mass	1896	kg
W_f	Vehicle front axle load	1052.3g	N
W_r	Vehicle rear axle load	843.68g	N
I_z	Vehicle Inertia	3803	kgm ²
a	Distance of c. g. to the front axle	1.2682	m
b	Distance of c. g. to the rear axle	1.5816	m

III. MLATERAL CONTROLLER DESIGN

As can be seen in Fig. 2. the design of lateral controller entails the following tasks: (1) Construction of target trajectory, (2) computing curvature and feedback error signals with respect to the target trajectory, and (3) computation of feedforward controller and (4) computation of feedback controller.

A. Target Trajectory Construction

To reiterate [5], [6], consideration of GPS information of lead and preceding vehicles arises from the need to address string instability in the lateral direction - certainly, cross track errors should not amplify for ensuring safety. Fig. 4, illustrates a convoy, where the ego ACV (shown in purple color) has access to sampled position data of the ACVs ahead. The red and blue colored dots correspond respectively to the locations at which their position data was transmitted to other ACVs including the

ego ACV. The ego ACV receives this data, stores it and uses only the data that is within a distance L_{preview} ahead of it; this is shown in Fig. 4, as ego preview data; this data can be sorted in increasing order of distance from the ego ACV. let $(x_1^l, y_1^l), (x_2^l, y_2^l), \dots, (x_N^l, y_N^l)$ (corresponding to red dots in the ego preview data) denote the GPS data of lead vehicle; similarly, let $(x_1^p, y_1^p), (x_2^p, y_2^p), \dots, (x_M^p, y_M^p)$ denote the data corresponding to the preceding ACV. The problem is to construct a target trajectory as a circular arc spline approximation of the data at hand. Circular arc spline\footnote{A circular arc spline is a union of straight line segments and circular arcs so that the resulting curve is continuous with tangent defined everywhere but allows for piecewise constant curvature} is especially useful here because (1) a majority of US roads are built as circular arc splines [25] (2) computation of curvature and error signals (namely, cross track error, heading and heading rate errors) becomes easy.

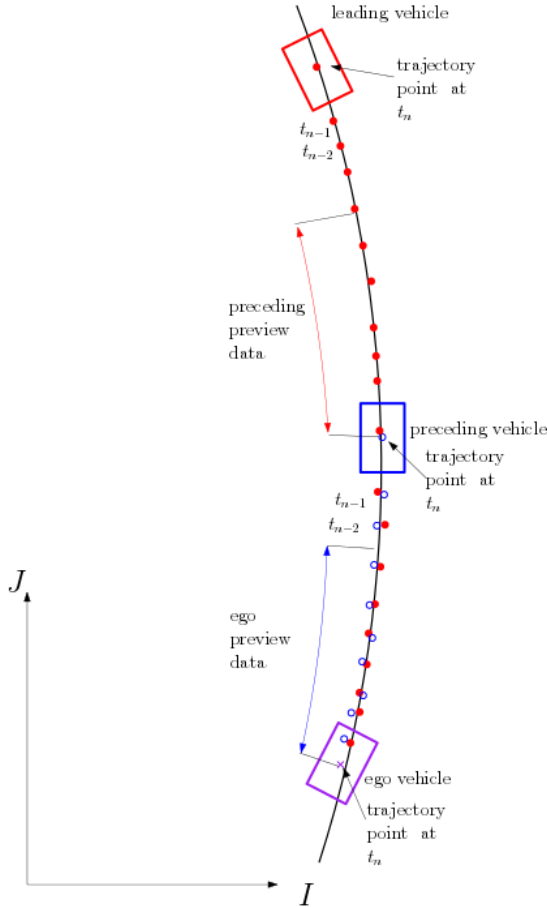


Fig. 4: Illustration of the sampled trajectories of ACVs in the convoy and the information available to the ego ACV

It has been mentioned in [1][24] that human drivers require a preview/lookahead information equivalent to about 0.8 sec of time headway; in other words, if v is the ACV's longitudinal speed, all the preview data within $L_{\text{preview}} = 0.8 \times v \approx 30$ m should suffice for highway speeds. Typically, the maximum frequency of GPS data update is 20 Hz and hence, $M, N < 20$. The duration for a lane change is typically 5 –

6 sec [26]; clearly, for this reason, it is reasonable to assume that there can be almost one change in curvature of the target trajectory in 1 sec. We currently use GPS-RTK [27] that has an accuracy of approximately 2 cm in position; correspondingly, the transmitted data is assumed to be of the same order of accuracy. Since the radius of curvature of the data is typically of the order of 100's of meters, and the distance between successive samples of GPS data transmitted by the ACVs is of the order of 1 m, it suffices to only consider circular arc splines where circular arcs and straight lines alternate in succession. Since the data is sorted and the GPS-RTK provides position data with a cm accuracy with the distance between successive data samples from ACV being of the order of m, we can exploit this situation further. For example, consider the case where the ego ACV that is going straight needs to decide whether to turn based on the available preview data. Since the data is sorted by distance, consider the data from the preceding vehicle (the same can be done for the lead vehicle also): Find the largest $k \geq 3$ such that points $(x_2^p, y_2^p), \dots, (x_{k-1}^p, y_{k-1}^p)$ are no farther than a threshold, say ϵ cm, from the line connecting (x_1^p, y_1^p) and (x_k^p, y_k^p) ; clearly, we can associate a straight line segment with the data $(x_1^p, y_1^p), \dots, (x_k^p, y_k^p)$ and associate a circular arc with the rest of the data. We choose the threshold to be 10 cm (about 5 times the accuracy specified by GPS-RTK). This would allow us to focus on circular arc approximation of the rest of data.

Since the preview data is available from lead ACV and preceding ACV, there are two possible architectures:

- Synthesize a composite ELC trajectory that fuses the GPS information of both lead and preceding vehicles of every following vehicle in the convoy.
- Synthesize two ELC trajectories with each trajectory corresponding to the information from a specific ACV (here lead or preceding ACV). One must then correspondingly synthesize feedback information to regulate the tracking error.

A general formulation for fitting a circular arc that would suffice for these two possible architectures will be considered in the next subsection.

Fitting a circular arc based on preview data

There are two sources for the preview data -- lead ACV and the preceding ACV; one may want to weigh the data differently. For this case, consider a weighing parameter $\alpha \in [0,1]$ that will be used in defining a convex combination of two different error functions.

Let (X_c, Y_c) be the coordinates of the center of the circle sought and R be its radius.

A circle is defined by an equation of the form:

$$e(x, y) = 0$$

where

$$e(x, y) := (x - X_c)^2 + (y - Y_c)^2 - R^2.$$

One can think of πe as the difference between the areas of a circle passing through a point (x, y) with center at (X_c, Y_c) and another circle of radius R . Associated with the given data,

$(x_1^p, y_1^p), \dots, (x_M^p, y_M^p), (x_1^l, y_1^l), \dots, (x_N^l, y_N^l)$, one can define a composite error

$$J = \alpha \sum_{i=1}^M (e(x_i^p, y_i^p))^2 + (1 - \alpha) \sum_{j=1}^N (e(x_j^l, y_j^l))^2$$

Then $(X_c, Y_c), R$ can be determined as the arguments minimizing J and can be determined from three linear equations in $X_c, Y_c, (R^2 - X_c^2 - Y_c^2)$.

In the first architecture, we pick $\alpha = 0.5$, i.e., we provide equal weight to the data from lead and preceding ACVs and then determine the composite ELC trajectory. The choice of $\alpha = 0.5$ simplifies implementation as we can treat the data from lead and preceding ACVs as coming from the same source ACV.

In the second architecture, we can set $\alpha = 1$ to compute a target trajectory based on the data associated with preceding ACV and $\alpha = 0$ to compute another target trajectory based on the data associated with lead ACV.

Once an ELC trajectory is computed, one must now calculate the feedback signals: the lateral error of the vehicle from the trajectory, e_{lat} , the heading error of the vehicle, $\tilde{\theta}$, and the heading rate error, $\dot{\tilde{\theta}}$. The radius of curvature allows us to compute the feedforward control with respect to an ELC trajectory and the feedback signals help vehicle track the trajectory!

B. Computation of Feedback Error Signals

Let (X_v, Y_v) denote ego ACV's position. Computation of feedback error signals depends on whether the trajectory represented by preview data is a straight-line segment or a circular arc. In the former case, the desired heading rate is zero; as can be seen from the illustration below, the lateral error can be computed to be:

$$e_{lat} = \frac{Y_v - mX_v - c}{\sqrt{1 + m^2}}$$

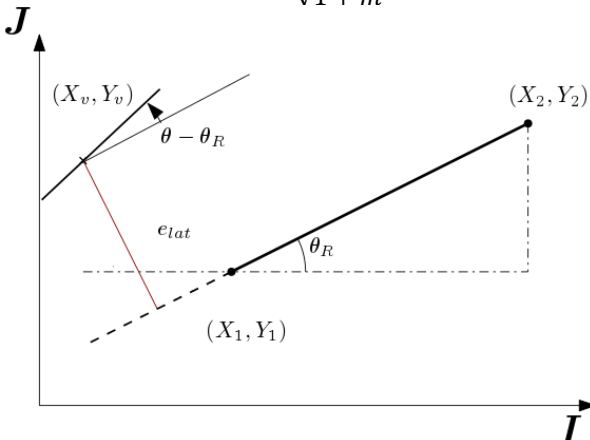


Fig. 5: Heading and lateral errors for a straight-line segment

where $y = mx + c$ is the straight line equation based on closest point (X_1, Y_1) and second closest point (X_2, Y_2) .

Desired yaw angle θ_R is also based on these two points. The yaw error is given by

$$\tilde{\theta} := \theta - \theta_R,$$

and the yaw rate error is given by:

$$\dot{\tilde{\theta}} := \dot{\theta}.$$

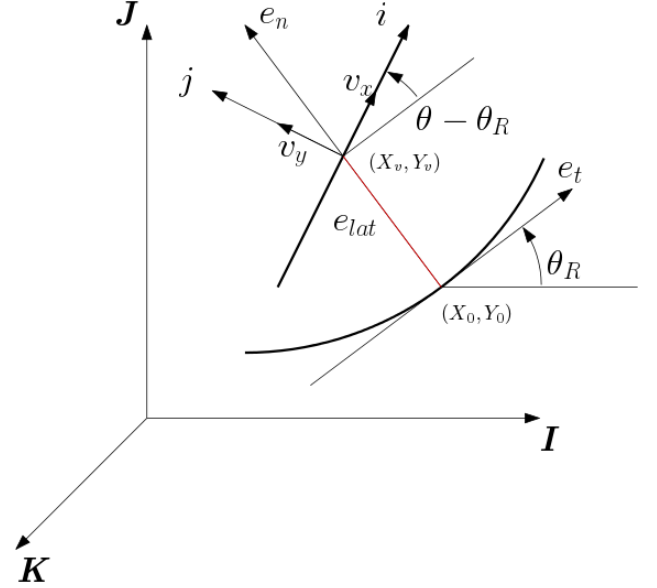


Fig. 6: Heading and lateral errors for a circular arc

If the trajectory is a circular arc, then the projection of (X_0, Y_0) onto the circular arc can be constructed by drawing a line joining the center of the circle (X_c, Y_c) to current position of the vehicle (X_v, Y_v) and extending, if necessary, to meet the circular arc at (X_0, Y_0) . The angle made by the tangent at (X_0, Y_0) with positive X axis of the ground will be represented by θ_R . As shown, unit vectors i, j are attached to the vehicle along the longitudinal and lateral axes respectively and the angle θ made by i with I represents the heading θ in the governing equations of motion.

The lateral error can be defined as:

$$e_{lat} := R - \sqrt{(X_v - X_c)^2 + (Y_v - Y_c)^2},$$

The yaw error can be defined as:

$$\tilde{\theta} := \theta - \theta_R$$

where θ_R is defined as based on closest point and second closest point on preview section. Correspondingly, the yaw rate error is:

$$\dot{\tilde{\theta}} := \dot{\theta} - \frac{v_x}{R}.$$

C. Feedforward Controller Synthesis

Lateral controller for tracking a trajectory can be decomposed into two parts: a feedforward part and a feedback part, i.e.,

$$\delta_c = \delta_{ff} + \delta_{fb}.$$

In the following subsections, we will outline how these controller components are designed:

D. Feedforward controller

Feedforward controller structure depends on the architecture employed.

1) With a Composite ELC Trajectory

In this case, there is only a single trajectory.

Feedforward controller essentially provides the steering input that would keep an ACV on a circular trajectory without any feedback if the initial conditions were to be appropriate and if the disturbance inputs were to be absent. One may view the feedforward steering input, δ_{ff} , as that steering input which results in the ACV's trajectory being a circle of radius R when it is traveling at a longitudinal speed of V_0 .

Clearly, the corresponding feedforward steering input is:

$$\delta_{ff} = \frac{a+b}{R} + K_{sg} \frac{V_0^2}{R}.$$

Note that for understeered vehicles, $K_{sg} > 0$ and the open-loop handling dynamics will be unconditionally stable [28][29].

2) Separate ELC trajectories based on lead and preceding ACVs

Let $\alpha \in [0,1]$ denote the weight we assign to the preview data from preceding ACV in terms of tracking. Then

$$\delta_{ff} = \alpha \left(\frac{a+b}{R_p} + K_{sg} \frac{V_0^2}{R_p} \right) + (1-\alpha) \left(\frac{a+b}{R_l} + K_{sg} \frac{V_0^2}{R_l} \right),$$

where R_l, R_p denote respectively the radii of trajectory computed based on the preview data of lead and preceding ACVs respectively.

E. Feedback Controller Design

As with feedforward controller design, feedback controller design also depends on the architecture.

1) Composite ELC trajectory

Feedback control is based on available information, namely, the errors e_{lat} , $\tilde{\theta}$ and $\dot{\tilde{\theta}}$ with respect to the composite ELC trajectory; the lateral velocity information is not readily available; hence, we seek a control law of the form:

$$\delta_{fb} = -k_e e_{lat} - k_\theta \tilde{\theta} - k_w \dot{\tilde{\theta}}$$

where the gains k_e, k_θ and k_w need to be determined.

2) Separate ELC trajectories corresponding to lead and preceding vehicle's preview data

Suppose $e_{lat,l}, \tilde{\theta}_l$ and $\dot{\tilde{\theta}}_l$ be the lateral spacing error, heading error and yaw rate error corresponding to the ELC trajectory based on lead ACV's data; similarly, $e_{lat,p}, \tilde{\theta}_p$ and $\dot{\tilde{\theta}}_p$ be corresponding errors for the ELC trajectory based on preview data from preceding ACV.

The structure of feedback controller we pick in this case is as follows:

$$\delta_{fb} = -(1-\alpha) \left(k_e e_{lat,l} + k_\theta \tilde{\theta}_l + k_w \dot{\tilde{\theta}}_l \right) - \alpha \left(k_e e_{lat,p} + k_\theta \tilde{\theta}_p + k_w \dot{\tilde{\theta}}_p \right).$$

F. Construction of the set of stabilizing structured Feedback Controllers

The gains k_e, k_θ and k_w must be chosen for implementation; in this subsection, we will adopt the

procedure from our earlier work on the construction of structured feedback controllers to arrive at the set for both cases.

1) With a Composite ELC trajectory:

We use the D-decomposition method from our earlier work[5] [17] to synthesize the set of stabilizing feedback gains.

From the governing equations, the transfer functions relating $e_{lat}(s), \tilde{\theta}(s)$ to $\delta_f(s)$ can be related through the open-loop characteristic polynomial $\Delta_o(s)$, as:

$$\Delta_o(s) = s^2 \left(mI s^2 + \frac{(I + ma^2)C_f + (I + mb^2)C_r}{V_0} s + \frac{(a+b)^2 C_f C_r}{V_0^2} - m(aC_f - bC_r) \right)$$

$$\frac{e_{lat}(s)}{\delta_f(s)} = \frac{C_f}{\Delta_o(s)} \left(I s^2 + \frac{b(b+a)C_r}{V_0} + (a+b)C_r \right)$$

$$\frac{\tilde{\theta}(s)}{\delta_f(s)} = \frac{C_f}{\Delta_o(s)} \left(mas^2 + \frac{(a+b)C_r}{V_0} s \right)$$

Since

$$\delta_f = H_{a(s)\delta_c(s)} = -H_a(s) \left(k_e e_{lat}(s) + (k_\theta + k_w s) \tilde{\theta}(s) \right),$$

it follows that the closed-loop characteristic equation can be expressed as:

$$\Delta_o(s) + H_a(s) k_e C_f \left(I s^2 + \frac{b(a+b)C_r}{V_0} s + (a+b)C_r \right) + H_a(s) (k_\theta + k_w s) C_f \left(mas^2 + \frac{(a+b)C_r}{V_0} s \right) = 0.$$

For the second-order steering actuation model, it follows that the characteristic polynomial may be expressed in terms of the control parameter vector $K = (k_e, k_\theta, k_w)$ as:

$$\Delta(s; K) = (J_w s^2 + b_w s + K_r) \Delta_o(s) + k_e K_r C_f \left(I s^2 + \frac{\{b(a+b)C_r\}}{V_0} s + (a+b)C_r \right) + (k_\theta + k_w s) K_r C_f \left(mas^2 + \frac{(a+b)C_r}{V_0} s \right)$$

2) With separate ELC trajectories based on preview data of preceding and lead vehicles

One can examine the evolution of $e_{lat,p}$ and apply the feedforward and feedback control inputs specified in the earlier subsections for this case. We can rewrite the feedback law as:

$$\delta_{fb} = -k_e e_{lat,p} + k_p \tilde{\theta}_p + k_\omega \dot{\tilde{\theta}}_p + \alpha \left(k_e (e_{lat,p} - e_{lat,l}) + k_\theta (\tilde{\theta}_p - \tilde{\theta}_l) + k_\omega (\dot{\tilde{\theta}}_p - \dot{\tilde{\theta}}_l) \right).$$

One may neglect the component of state $(e_{lat,p}, \tilde{\theta}_p, \dot{\tilde{\theta}}_p)$ in the terms $e_{lat,p} - e_{lat,l}, \tilde{\theta}_p - \tilde{\theta}_l$ and $\dot{\tilde{\theta}}_p - \dot{\tilde{\theta}}_l$ as these will be dominated by the difference in the ELC trajectories constructed based on preview data of lead and preceding ACVs. For this reason, the characteristic polynomial will remain the same as before.

Hence, a natural problem regarding stability of tracking is to determine the set of control gains, K , so that the closed loop characteristic polynomial (9) is Hurwitz. An advantage of determining the entire set is that the set can be pruned to accommodate additional performance criteria.

3) Construction of the set of stabilizing fixed structure controllers

There are many ways to construct the set of controllers [30]-[33] in the parameter space. We adopt the D-decomposition approach of [31][33] here; essentially, this approach relies on the continuous dependence of roots of a polynomial on its coefficients for every regular perturbation. The approach then involves decomposing the parameter space into disjoint signature-invariant regions by identifying their boundaries. The boundaries can be obtained by (a) determining the set of K for which $\Delta(0, K) = 0$ and (b) determining the set of K for which $\Delta(j\omega, K) = 0$ for some ω . Once the parameter space is partitioned, one can then sample every partition to determine the partition corresponding to $\Delta(s; K)$ being Hurwitz.

Note that $\Delta(s, K) = A_6 s^6 + A_5 s^5 + A_4 s^4 + A_3 s^3 + A_2 s^2 + A_1 s + A_0$, where

$$\begin{aligned} A_6 &= \frac{Im}{\omega_n^2}, \\ A_5 &= \frac{2Im\zeta}{\omega_n} + \frac{C_f(I + a^2m) + C_r(I + b^2m)}{V_0\omega_n^2}, \\ A_4 &= \frac{2\zeta(C_f(I + a^2m) + C_r(I + b^2m))}{V_0\omega_n} \\ &\quad + \left(\frac{(a+b)^2 C_f C_r}{V_0^2 \omega_n^2} - m(aC_f - bC_r) \right) \\ &\quad + mI, \\ A_3 &= \left(\frac{2\zeta((a+b)^2 C_f C_r)}{V_0^2 \omega_n} - m(aC_f - bC_r) \right) \\ &\quad + \frac{C_f(I + a^2m) + C_r(I + b^2m)}{V_0} + C_f m a k_\omega, \\ A_2 &= \left(\frac{(a+b)^2 C_f C_r}{V_0^2} - m(aC_f - bC_r) \right) \\ &\quad + \left(C_f I k_e + C_f C_r \frac{(a+b)}{V_0} k_\omega + m a C_f k_\theta \right), \\ A_1 &= C_f C_r \frac{(a+b)}{V_0} (b k_e + k_\theta), \\ A_0 &= C_f C_r (a+b) k_e, \end{aligned}$$

where ζ, ω_n are the damping ratio and natural frequency of steering actuation. They can be found out in our previous work[17][24].

It is important to note the set of stabilizing controllers is specific to the operating speed V_0 as the coefficients $A_0, A_1, A_2, A_3, A_4, A_5, A_6$ depend *quadratically* on $\frac{1}{V_0}$. Define

a parameter $\gamma := \frac{1}{V_0}$; one can then construct the set of stabilizing controller for each $\gamma \in \left[\frac{1}{V_{min}}, \frac{1}{V_{max}} \right]$, where V_{min}, V_{max} are the limiting values of the operating longitudinal speeds. We then choose a control gain vector $K = (k_e, k_\theta, k_\omega)$ that lies in the intersection as γ varies from $\frac{1}{V_{max}}$ to $\frac{1}{V_{min}}$.

There is one detail that one must take care in this approach. In the construction of the set of stabilizing controllers, γ has been considered as a parameter that remains constant; however, the governing equations were simplified based on the condition that the longitudinal speed is a constant. If the rate of change of longitudinal speed is sufficiently small, it is intuitive that guarantees of closed loop stability will continue to hold following the techniques of slowly varying parameter systems as described in Section 9.3 of [34]. We will provide a similar bound here on the longitudinal acceleration of a vehicle performing the ELC for closed-loop stability guaranteed to hold.

G. Closed-loop Stability with varying longitudinal velocity

Let Q, G, H be appropriate matrices (in controllable canonical form) so that the the transfer function, $H_a(s)$, from steering command, δ_c , to steering angle, δ_f , has the following minimal realization:

$$\dot{\eta} = Q\eta + G\delta_c, \quad \delta_f = H\eta.$$

Note that the dynamics of the vehicle can be expressed as

$$\begin{pmatrix} \dot{x} \\ \dot{x} \end{pmatrix} = \begin{pmatrix} 0 & I \\ -L & -\gamma C_0 \end{pmatrix} \begin{pmatrix} x \\ \dot{x} \end{pmatrix} + \begin{pmatrix} 0 \\ B \end{pmatrix} C_f \delta_f - \begin{pmatrix} 0 \\ F \end{pmatrix} \frac{1}{R}$$

Let $K_p := [k_e \ k_\theta]$ and $K_v := [0 \ k_\omega]$.

Since $\delta_c = -K_p x - K_v \dot{x}$,

the closed loop dynamics is then given by:

$$\underbrace{\begin{pmatrix} \dot{x} \\ \dot{x} \\ \dot{\eta} \end{pmatrix}}_z = \underbrace{\begin{pmatrix} 0 & I & 0 \\ -L & -\gamma C_0 & B H C_f \\ -G K_p & -G K_v & Q \end{pmatrix}}_{\hat{A}(\gamma)} \underbrace{\begin{pmatrix} x \\ \dot{x} \\ \eta \end{pmatrix}}_z + \underbrace{\begin{pmatrix} 0 \\ -F \\ 0 \end{pmatrix}}_{\hat{F}} \frac{1}{R}$$

Once the controller gains are fixed, i.e., K_p, K_v are known, closed loop stability can be examined by formally considering a linear system $\dot{z} = A(t)z(t)$.

Problem (9.31) of [34] can be employed to establish closed loop stability; it is stated here for completeness:

Lemma 1: Suppose the linear system: $\dot{z} = A(t)z(t)$ satisfies the following conditions:

- For some $k > 0$, $|A(t)| \leq k$ for all $t \geq 0$,
- For some $\sigma > 0$, every eigenvalue of $A(t)$ has a real part less than $-\sigma$ for every $t \geq 0$, and
- $\|\dot{A}(t)\|$ is square integrable, i.e., for some $\rho > 0$,

$$\int_0^\infty \|\dot{A}(t)\|^2 dt \leq \rho.$$

Then, the equilibrium $z = 0$ is exponentially stable.

Proof: It can be found in the solutions manual [35].

Closed loop stability with varying longitudinal speed has not been considered in the literature; the following result provides the connection between “frozen parameter” control synthesis and stability of linear time varying system at hand with varying longitudinal speed:

Proposition 1: Consider the linear time varying system $\dot{z} = A(\gamma(t))z$ given above. Suppose K_p, K_v have been chosen to satisfy the following conditions:

- The real part of eigenvalues of $A(\gamma)$ are less than $-\sigma$ for every $\gamma \in \left[\frac{1}{v_{max}}, \frac{1}{v_{min}}\right]$.
- The longitudinal acceleration of the vehicle is square integrable, i.e.,

$$\int_0^\infty \dot{v}_x^2(\tau) d\tau < 0$$

Then, the equilibrium $z = 0$ is exponentially stable.

Proof: We will use the proof of Problem (9.31) of [34] to arrive at the result. Essentially, it requires that three conditions be satisfied:

- Note that $\gamma(t) = \frac{1}{v_x(t)}$. Hence, $|A(\gamma(t))|$ is bounded for all t or equivalently, it is bounded for all $\gamma \in \left[\frac{1}{v_{max}}, \frac{1}{v_{min}}\right]$; in this case, it is easy to verify that this condition holds.
- The real part of the eigenvalues of $A(\gamma(t))$ are less than $-\sigma$ for some $\sigma > 0$; again this condition holds because the gains K_p, K_v have been chosen to be in the set of stabilizing controllers that render $A(\gamma(t))$ Hurwitz for every $\gamma \in \left[\frac{1}{v_{max}}, \frac{1}{v_{min}}\right]$.
- The third condition requires $\int_0^\infty |\dot{A}(\gamma(\tau))|^2 d\tau < 0$; in our case, it is easy to see that $A(\gamma)$ is linear in γ and for some appropriate constant matrices A_0 and A_1 , we can express $A(\gamma) = A_0 + \gamma A_1$. Consequently, $\dot{A}(\gamma) = \dot{\gamma} A_1$,

implying that $\dot{A}(\gamma)$ is square integrable if $\dot{\gamma}$ is square integrable, i.e., $\dot{\gamma} \in L_2$ as γ is bounded.

However,

$$\begin{aligned} \dot{\gamma} &= -\frac{1}{v_x^2} \dot{v}_x \\ \Rightarrow \int_0^\infty |\dot{\gamma}(\tau)|^2 d\tau &= \int_0^\infty \frac{1}{v_x^4(\tau)} |\dot{v}_x(\tau)|^2 d\tau \\ &\leq \frac{1}{v_{min}^4} \int_0^\infty |\dot{v}_x(\tau)|^2 d\tau. \end{aligned}$$

By virtue of \dot{v}_x being square integrable, the third condition is also satisfied. Hence, the closed loop time varying system is exponentially stable by Lemma 1.

The assumption that the longitudinal acceleration is square integrable is very reasonable because often acceleration/deceleration maneuvers are associated with a finite change in longitudinal speed; the finite time duration of acceleration maneuvers renders this condition readily satisfied.

IV. NUMERICAL AND EXPERIMENTAL RESULTS

A. Construction of Stabilizing Set of Feedback Gains

In order to construct the set of stabilizing feedback gains, we used the parameters from Table II.

TABLE II
PARAMETERS OF VEHICLE

Parameter	Value	Unit
m	1896	[kg]
C_f	4000000	[N/rad]
C_r	381900	[N/rad]
I	3803	[kgm ²]
a	1.2682	[m]
b	1.5816	[m]
ζ	0.4056	[-]
ω_n	21.4813	[rad/sec]

Since the stabilizing set (which is non-convex) depends on V_0 , we find the sets of all the stabilizing controllers for a range of speeds in $\{10,20,30,40,50,60,67\}$ mph and selected a controller $(k_e, k_\theta, k_\omega) = (0.06, 0.96, 0.08)$ that belongs to the interior of the intersection of all these stabilizing sets. The stabilizing set corresponding to $V_0 = 30$ m/s is shown in Fig. 7. Since the stabilizing set is bounded, and the chosen set of gains is in the interior, a ball centered at the chosen controller can be completely inserted in the stabilizing set of controllers; this would automatically imply that condition (a) of Proposition 1 is satisfied, as eigenvalues of A are continuous functions of controller gains and the ball of stabilizing gains containing the chosen gains is bounded.

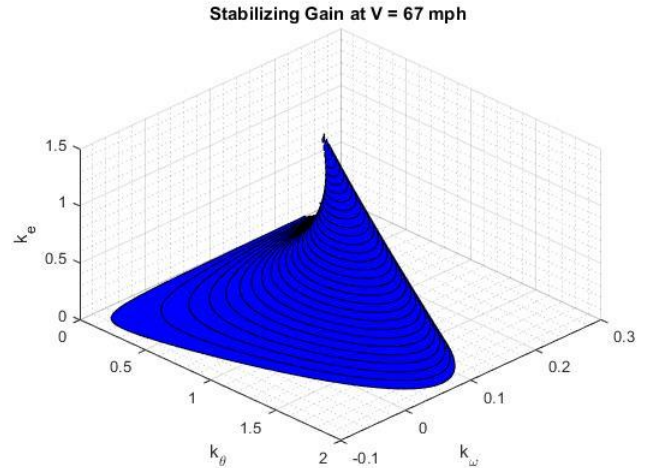


Fig. 7: Stabilizing set of controllers

B. Numerical Simulation Setup

The trajectory in Fig. 8 represents a nominal double lane change on a 1 km road section and is the target trajectory for lead ACV. It corresponds to an ACV turning left to go to the adjacent left lane and then right to get back into the original lane. The second ACV (literally, the first following ACV) in the convoy will use the sampled trajectory information of the

lead ACV and adopt the control law developed in this paper. All other vehicles in the platoon will have access to the sampled trajectory information of the lead and their preceding ACVs path and adopt the lateral controller designed in the earlier section; we test the two designs - one is based on the composite ELC trajectory, the other one is based on separate trajectory on lead and preceding vehicles. For simulations in this section, we consider a four-vehicle platoon. Every vehicle in the platoon maintains a constant speed of $30m/s$. Initially, all the vehicles have zero lateral value and zero heading error.

1) Lateral control with a composite ELC trajectory

For simplicity of implementation, α was chosen to be 0.5 in the computation of the composite ELC trajectory for each ACV.

Based on the composite ELC trajectory, feedforward control input, feedback error signals and feedback control have been determined as described in the controller synthesis section. Fig. 9 shows the lateral error response of the control scheme while trying to track the composite ELC trajectory in Fig. 8. In the double lane change maneuver considered, the first (left) lane change begins at around 8 seconds and ends before 15 seconds; the second (right) lane change begins at approximately 24 seconds and ends at 30 seconds. The maximum lateral error was found to be approximately 8 cm and occurred at the beginning and end of curved section of the trajectory; see Fig 9; moreover, the maximum lateral errors seem to form a monotonically decreasing sequence affirming lateral string stability.

2) Lateral control with separate ELC trajectories

In this section, consider the separate ELC trajectories, one based on the lead vehicle's data and the other based on preceding vehicle's data. As described in Section III, we design the feedback and feedforward controllers and weigh them equally, i.e., set $\alpha = 0.5$. The target paths is shown in Fig. 10. As shown in Fig. 11, the maximum lateral error of about 0.08 meters was obtained and occurred at the beginning and end turning section of lane change. Moreover, string instability was not observed in the simulations.

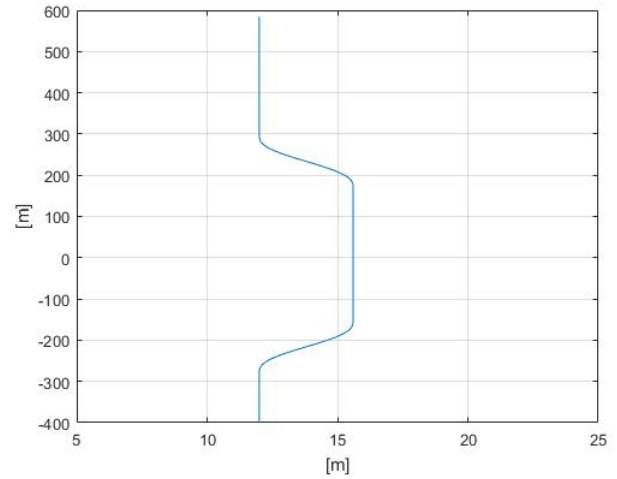


Fig. 8: Composite ELC Trajectory: Vehicle reference path

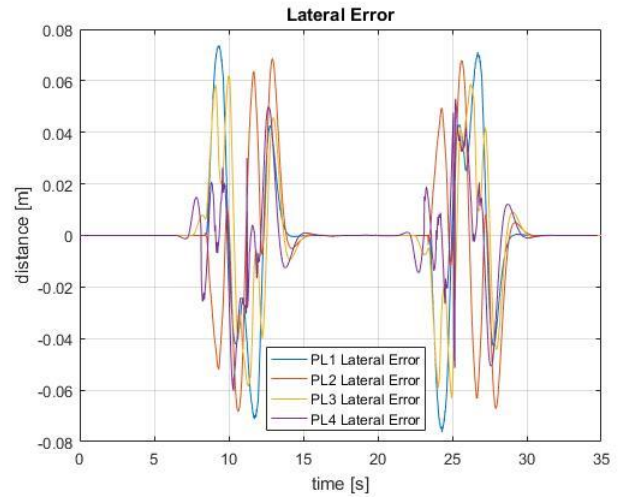


Fig. 9: Composite ELC Trajectory: Lateral error

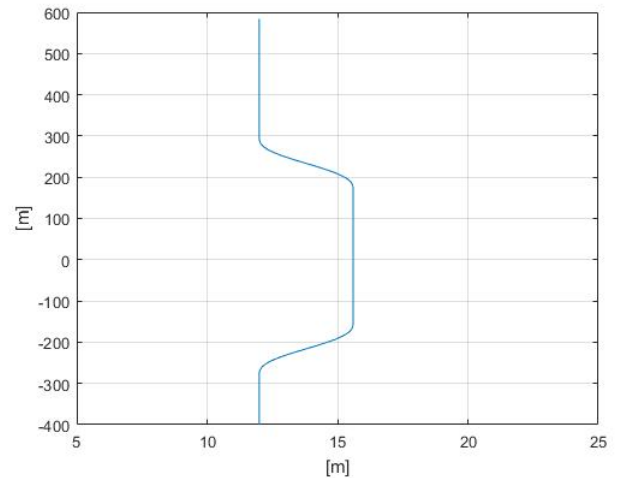


Fig. 10: Separate Trajectories: Vehicle reference path

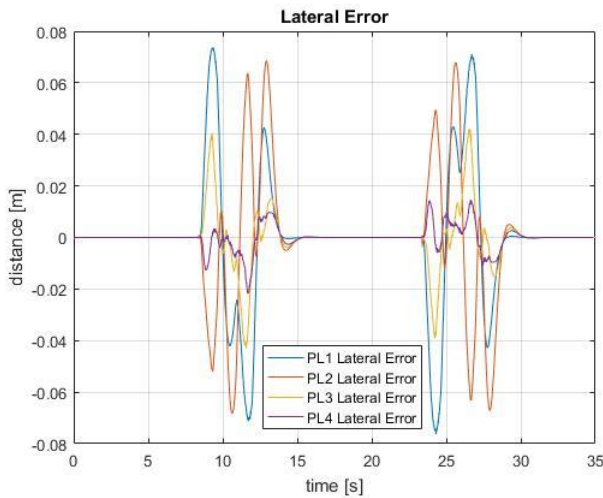


Fig. 11: Separate Trajectories: Lateral difference between vehicles and their preceding one's track

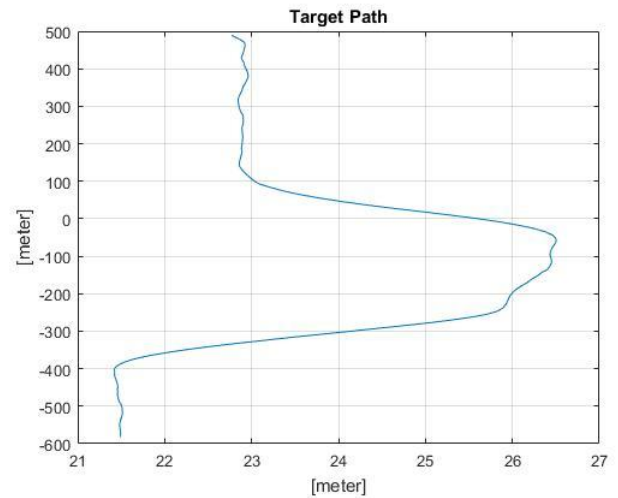


Fig. 12: Experiment: Vehicle reference path

C. Experimental Setup

The developed control algorithms were implemented on a Lincoln MKZ car. The vehicle was equipped with a drive-by wire system for autonomous steering, throttle and brake control. Data concerning the vehicle states (position, yaw angle, and yaw rate) were obtained from an on-board integrated GPS system and IMU unit. The controller operates at 50 Hz. Since we had only one Lincoln MKZ, we emulated a convoy with multiple runs of the same vehicle - this was possible because of the look-ahead nature of the control scheme as every following vehicle needed only the information of its preceding ACV and the lead ACV in the convoy. In the first run, the Lincoln MKZ vehicle would track the trajectory as a lead ACV in the convoy; the closed loop trajectory information (provided via time stamped GPS information) is stored on-board and accessed in subsequent runs. In the second run, it will access the stored GPS information from the first run to simulate the acquisition of perfectly communicated GPS information from the lead ACV; in the i^{th} run, it would access the stored trajectory information from the preceding run and the first run to compute the steering command.

In the experiment conducted on our RELLIS campus, the target speed of every vehicle in the platoon is 25 m/s. The target trajectory for the experiment is the same as the one considered in the numerical simulation section. *Due to the time limitation, we computed the steering angle using the first architecture described in this paper - which is based on composite ELC trajectory.* The desired trajectory is shown as Fig. 12.

D. String Stability with lead ACV's preview data

If the target trajectory for the following ACV incorporates the lead vehicle's position information, then lateral string stability was observed in Fig. 13.

The readers are encouraged to view the accompanying video at [url{https://youtu.be/UT1OYCb50gU}](https://youtu.be/UT1OYCb50gU)

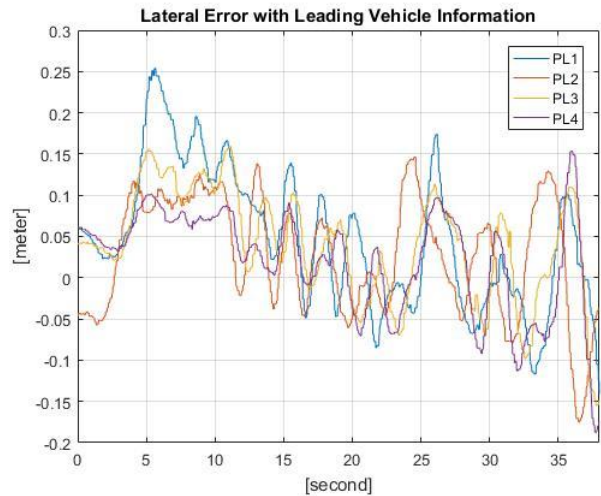


Fig. 13: Experiment: Lateral String Stability With Lead Vehicle's (Preview) Data

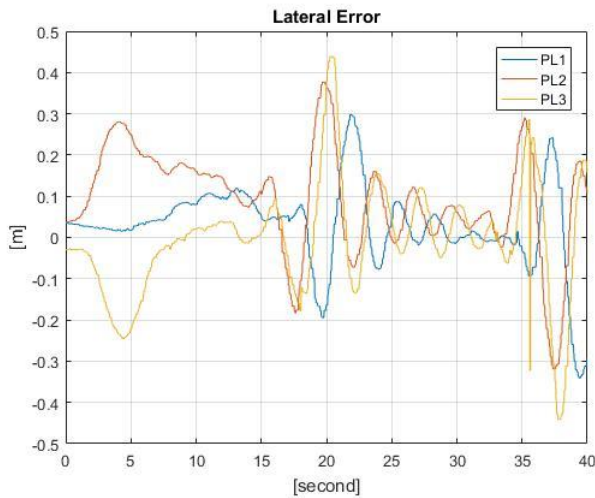


Fig. 14: Experiment: Lateral String Instability Without Lead Vehicle's (Preview) Data.

V. CONCLUSIONS

In this work, we considered the problem of controlling the lateral motion of a convoy of autonomous vehicles; lateral control of an autonomous following vehicle is based on the sampled GPS data from its lead and preceding vehicles. We presented two controller architectures to accommodate (and fuse) the communicated data. In either case, we considered data that corresponded to a position of the lead/preceding vehicle within a specified distance of the ego vehicle in the convoy. In the first architecture, a composite ELC trajectory was constructed as a circular arc spline by treating both data streams as if they originate from the same source. This is simpler in terms of implementation as there is only one trajectory to be computed and only one set of feedback errors and corresponding feedback and feedforward actions to be computed. In the second architecture, a trajectory each was constructed for each ego vehicle as a circular spline that corresponded to the data from its preceding and lead vehicles respectively. Two sets of feedback errors and control actions were then combined with appropriate weights to synthesize control actions. Simulation and experimental results corroborate the effectiveness of the control schemes. The second scheme was found to be slightly better in terms of its performance in simulation; experimentation will be conducted in the near future once the prevailing COVID restrictions on experimentation are relaxed. In simulations, and in the experimental tests conducted so far, string instability was not observed thus far.

VI. DISCLAIMER

The contents of this report reflect the views of the authors, who are responsible for the facts and the accuracy of the information presented herein. This document is disseminated in the interest of information exchange. The report is funded, partially or entirely, by a grant from the U.S. Department of Transportation's University Transportation Centers Program. However, the U.S. Government assumes no liability for the contents or use thereof.

VII. ACKNOWLEDGMENT

Support for this research was provided in part by a grant from the U.S. Department of Transportation, University Transportation Centers Program to the Safety through Disruption University Transportation Center (451453-19C36).

REFERENCES

- [1] J.H.H.M. Alleleijn and Henk Nijmeijer and Sinan Oncu and Jeroen Ploeg, "Lateral string stability of vehicle platoons," in D & C Eindhoven University of Technology, Internship report, 2014.
- [2] R. Fenton and G. Melocik and K. Olson, IEEE Transactions on Automatic Control, On the steering of automated vehicles: Theory and experiment, 1976, Volume 21, Number 3, Pages 306-315,
- [3] Peng, Huei and Zhang, Weibin and Shladover, Steven and Tamizuka, Masayoshi and Aral, Alan. "Magnetic-marker-based lane keeping: a robustness experimental study", 1993, SAE Technical Paper.
- [4] J. Taylor, J. Kosecka, R. Blasi, and J. Malik, "A comparative study of vision-based lateral control strategies for autonomous highway driving," The International Journal of Robotics Research, vol. 18, no. 5, pp. 442-453, 1999. [Online]. Available: <https://doi.org/10.1177/027836499901800502>
- [5] M. Liu, S. Rathinam, and S. Darbha, "Lateral control of a convoy of vehicles with a limited preview information," in Artificial Intelligence and Machine Learning for Multi-Domain Operations Applications II, T. Pham, L. Solomon, and K. Rainey, Eds., vol. 11413, International Society for Optics and Photonics. SPIE, 2020, pp. 547 - 558. [Online]. Available: <https://doi.org/10.1117/12.2558737>
- [6] Guang Lu and M. Tomizuka, "A practical solution to the string stability problem in autonomous vehicle following," in Proceedings of the 2004 American Control Conference, vol. 1, 2004, pp. 780-785 vol.1.
- [7] O. Hassanain, M. Alirezai, J. Ploeg, and N. van de Wouw, "String-stable automated steering in cooperative driving applications," Vehicle System Dynamics, vol. 58, no. 5, pp. 826-842, 2020. [Online]. Available: <https://doi.org/10.1080/00423114.2020.1749288>
- [8] D. Swaroop and J. K. Hedrick, "String stability of interconnected systems," IEEE Transactions on Automatic Control, vol. 41, no. 3, pp.349-357, 1996.
- [9] S. K. Gehrig and F. J. Stein, "A trajectory-based approach for the lateral control of car following systems," in SMC'98 Conference Proceedings. 1998 IEEE International Conference on Systems, Man, and Cybernetics (Cat. No.98CH36218), vol. 4, 1998, pp. 3596-3601 vol.4.
- [10] O. Hassanain, M. Alirezai, J. Ploeg, and N. van de Wouw, "String-stable automated steering in cooperative driving applications," Vehicle System Dynamics, vol. 58, no. 5, pp. 826-842, 2020. [Online]. Available: <https://doi.org/10.1080/00423114.2020.1749288>
- [11] D. Bevil, X. Cao, M. Gordon, G. Ozbilgin, D. Kari, B. Nelson, J. Woodruff, M. Barth, C. Murray, A. Kurt, K. Redmill, and U. Ozguner, "Lane change and merge maneuvers for connected and automated vehicles: A survey," IEEE Transactions on Intelligent Vehicles, vol. 1, no. 1, pp. 105-120, 2016.
- [12] S. E. Shladover, C. A. Desoer, J. K. Hedrick, M. Tomizuka, J. Walrand, W. Zhang, D. H. McMahon, H. Peng, S. Sheikholeslam, and N. McKeown, "Automated vehicle control developments in the path program," IEEE Transactions on Vehicular Technology, vol. 40, no. 1, pp. 114-130, 1991.
- [13] S. E. Shladover, "Review of the state of development of advanced vehicle control systems (avcs)," Vehicle System Dynamics, vol. 24, no. 6-7, pp. 551-595, 1995. [Online]. Available: <https://doi.org/10.1080/00423119508969108>
- [14] H. Peng and M. Tomizuka, "Preview control for vehicle lateral guidance in highway automation. Journal of Dynamic Systems, Measurement, and Control, vol. 4, no. 115, pp. 679-689, 1993.
- [15] Han-Shue Tan, J. Guldner, S. Patwardhan, Chieh Chen, and B. Bougler, "Development of an automated steering vehicle based on roadway magnets-a case study of mechatronic system design," IEEE/ASME Transactions on Mechatronics, vol. 4, no. 3, pp. 258-272, 1999.
- [16] T. Fujioka and M. Omac, "Vehicle following control in lateral direction for platooning," Vehicle System Dynamics, vol. 29, no. SUPPL., pp.422-437, Dec. 1998.
- [17] M. Liu, S. Rathinam, and S. Darbha, "Lateral control of an autonomous car with limited preview information," in 18th European Control Conference (ECC), 2019, pp. 3192-3197.

- [18] S. E. Shladover, C. A. Desoer, J. K. Hedrick, M. Tomizuka, J. Walrand, W. Zhang, D. H. McMahon, H. Peng, S. Sheikholeslam, and N. McKeown, "Automated vehicle control developments in the path program," *IEEE Transactions on Vehicular Technology*, vol. 40, no. 1, pp. 114–130, 1991.
- [19] H. Guldner, J.; Tan and S. Patwardhan, "Analysis of automatic steering control for highway vehicles with look-down lateral reference systems," *Vehicle System Dynamics*, vol. 26, no. 4, pp. 243–269, 1996.
- [20] P. Hingwe and M. Tomizuka, "Experimental evaluation of a chatter free sliding mode control for lateral control in ahs," in *Proceedings of the 1997 American Control Conference (Cat. No.97CH36041)*, vol. 5, no. 5, 1997, pp. 3365–3369.
- [21] Wonshik Chee, M. Tomizuka, S. Patwardhan, and Wei-Bin Zhang, "Experimental study of lane change maneuver for ahs applications," in *Proceedings of American Control Conference*, vol. 1, no. 1, 1995, pp. 139–143.
- [22] H. A. Pham and J. K. Hedrick, "A robust optimal lateral vehicle control strategy," in *Proceeding of the IEEE International Conference on Control Applications held together with IEEE International Symposium on Intelligent Control*, vol. 1, no. 1, 1996, pp. 361–366.
- [23] N. Kapania and J. Gerdes, "Design of a feedback-feedforward steering controller for accurate path tracking and stability at the limits of handling." *Vehicle System Dynamics*, vol. 53, no. 12, pp. 1687–1704, 2015.
- [24] M. Liu, S. Rathinam, and S. Darbha, "Lateral control of an autonomous and connected vehicle with limited preview information," *IEEE Transactions on Intelligent Vehicles*, 2020, under review.
- [25] R. L. Cheu, "Highway geometric design," in *The Handbook of Highway Engineering*, 1st ed., T. F. Fwa, Ed. CRC Taylor & Francis Group, 2006, ch. 6, pp. 1–15.
- [26] T. Toledo and D. Zohar, "Modeling duration of lane changes," *Transportation Research Record*, vol. 1999, no. 1, pp. 71–78, 2007. [Online]. Available: <https://doi.org/10.3141/1999-08>
- [27] Piksi Multi-Product Summary. [Online]. Available: <https://www.swiftnav.com/sites/default/files/piksimultiproductsummar.pdf>
- [28] L. Segel, "An investigation of automobile handling as implemented by a variable-steering automobile. "Human Factors: The Journal of the Human Factors and Ergonomics Society, vol. 6, no. 4, pp. 333–341, 1964.
- [29] D. Crolla and D. Cao, "The impact of hybrid and electric powertrains on vehicle dynamics, control systems and energy regeneration." *Vehicle System Dynamics*, vol. 50, pp. 95–109, 2012.
- [30] W. Malik, Darbha, S., and Bhattacharyya, S., "A linear programming approach to the synthesis of fixed-structure controllers." *IEEE Transactions on Automatic Control*, vol. 53, no. 6, pp. 1341–1352, 2008.
- [31] S. P. Bhattacharyya, Datta, A., and Keel, L. H., *Linear control theory: structure, robustness, and optimization*. CRC press, 2018.
- [32] M. Henrion, D.; Sebek and V. Kucera, "Positive polynomials and robust stabilization with fixed-order controllers." *IEEE Transactions on Automatic Control*, vol. 48, no. 7, pp. 1178–1186, 2003.
- [33] D. D. Siljak, "Parameter space methods for robust control design: a guided tour." *IEEE Transactions on Automatic Control*, vol. 34, no. 7, pp. 674–688, 1989.
- [34] H. K. Khalil and J. W. Grizzle, *Nonlinear systems*. Prentice hall Upper Saddle River, NJ, 2002, vol. 3.
- [35] H. K. Khalil, *Nonlinear systems: solution manual*. New York: Macmillan., 1992, vol. 3